Nyembezi Dhliwayo,[1] Michael P. Sarras Jr.,[2] Ernest Luczkowski,[1] Samantha M. Mason,[1] and Robert V. Intine[1,2]

Parp Inhibition Prevents Ten-Eleven Translocase Enzyme Activation and Hyperglycemia-Induced DNA Demethylation

Diabetes 2014;63:3069–3076 | DOI: 10.2337/db13-1916

Studies from human cells, rats, and zebrafish have documented that hyperglycemia (HG) induces the demethylation of specific cytosines throughout the genome. We previously documented that a subset of these changes become permanent and may provide, in part, a mechanism for the persistence of complications referred to as the metabolic memory phenomenon. In this report, we present studies aimed at elucidating the molecular machinery that is responsible for the HG-induced DNA demethylation observed. To this end, RNA expression and enzymatic activity assays indicate that the ten-eleven translocation (Tet) family of enzymes are activated by HG. Furthermore, through the detection of intermediates generated via conversion of 5-methylcytosine back to the unmethylated form, the data were consistent with the use of the Tet-dependent iterative oxidation pathway. In addition, evidence is provided that the activity of the poly(ADP-ribose) polymerase (Parp) enzyme is required for activation of Tet activity because the use of a Parp inhibitor prevented demethylation of specific loci and the accumulation of Tet-induced intermediates. Remarkably, this inhibition was accompanied by a complete restoration of the tissue regeneration deficit that is also induced by HG. The ultimate goal of this work is to provide potential new avenues for therapeutic discovery.

Diabetes mellitus (DM) currently affects 285 million individuals worldwide, and this is projected to increase to 439 million by 2030 (1). Evidence from the laboratory (2–7) and large-scale clinical trials (8–18) has revealed that diabetes complications progress unimpeded via the phenomenon of "metabolic memory" (MM), even when glycemic control is pharmaceutically reestablished (19,20). Epigenetic mechanisms are the primary method that confer the ability of cells and organs to "memorize" previous environmental conditions and, hence, are assumed to be significant mechanisms supporting MM. Variations in "normal" DNA methylation are correlated with many aspects of DM, including susceptibility (21–23), insulin resistance (24), diabetes complication development (25), and early detection (26–28). Very recently, a comprehensive genomic DNA methylation profiling of type 2 DM islets revealed that CpG loci displayed a significant hypomethylation phenotype and may provide insight on diabetic islets and disease pathogenesis (29). The first report demonstrating a cause-and-effect relationship between hyperglycemia (HG) and altered DNA methylation documented that genomic hypomethylation was induced within the liver of type 1 DM rats as early as 2 weeks after HG onset (30). Pirola et al. (31) examined human primary aortic endothelial cells exposed to high glucose (24 h) in vitro and performed a more comprehensive analysis of histone acetylation and DNA methylation. In this study, they observed significant alterations in DNA methylation patterns and showed that induced methylation changes localized to regions within 5 kBs of transcriptional start sites. They also observed broad

[1]Dr. William M. Scholl College of Podiatric Medicine, Rosalind Franklin University of Medicine and Science, North Chicago, IL
[2]Department of Cell Biology and Anatomy, Chicago Medical School, Rosalind Franklin University of Medicine and Science, North Chicago, IL
Corresponding author: Robert V. Intine, robert.intine@rosalindfranklin.edu.
Received 19 December 2013 and accepted 1 April 2014.

This article contains Supplementary Data online at http://diabetes.diabetesjournals.org/lookup/suppl/doi:10.2337/db13-1916/-/DC1.

© 2014 by the American Diabetes Association. Readers may use this article as long as the work is properly cited, the use is educational and not for profit, and the work is not altered.

See accompanying article, p. 2906.

changes to H3K9/K14 acetylation and reported that regionalized hyperacetylation correlated well with DNA hypomethylation and HG-induced gene induction. However, these studies did not examine MM to determine the persistence of these changes.

We recently reported the use of a zebrafish model where an induced HG state (DM) can be subsequently resolved such that the fish return to euglycemia (MM) (7). This model provides a unique opportunity to examine HG-induced changes within a wide variety of tissues as the fish transverse through the normal, DM, and MM states. Importantly, this model is useful for the study of important regulatory systems underlying the DM and MM states and defining the molecular relationship between the two. We have used this model to document that the complications of impaired limb (caudal fin) regeneration and impaired skin wound healing continued after restoration of euglycemia. Moreover, through methylated DNA immunoprecipitation, followed by sequencing experiments, we documented that HG induces specific cytosine–phosphate–guanine (CpG) island demethylation that persists for most loci in the MM state. When these data were viewed within the context of global gene expression, a correlation of CpG island DNA demethylation changes and altered expression was observed. Therefore, the persistence of the HG-induced tissue regeneration capacity correlated directly with induced DNA demethylation, and this correlated with persistent gene expression alterations in the MM state. From this we concluded that the epigenetic DNA methylation mechanism may be partly responsible for the MM phenomenon.

Until recently, CpG methylation has been viewed as a stable epigenetic modification that could only be reversed passively through DNA replication, presumably via a reduction of DNA methyltransferase activity. However, this idea has been challenged because active cytosine demethylation is associated with several stages of development, neuronal memory, differentiation of pluripotent stem cells, and several human disorders (32–35). A number of DNA demethylation mechanisms, which share components, have been proposed, and all require further modification of 5-methyl-cytosine (5mC) at the amine group or at the methyl group (Fig. 1) (33,34). In the first of these, the growth-arrest and DNA damage-inducible (Gadd45) family acts as an adapter to recruit the Aid/Apobec (activation-induced cytidine deaminase/apolipoprotein B mRNA-editing enzyme) complex, which deaminates 5mC and converts it to thymine (Fig. 1). The other two proposed mechanisms are initiated by the ten–eleven translocation family (Tet1,2,3) of Fe(II)/2-oxoglutarate-dependent dioxygenases, which oxidize 5mC to produce 5-hydroxymethyl-cytosine (5hmC) (36,37).

Once 5hmC is formed, two separate pathways may be taken to convert 5hmC back into cytosine. In the first, iterative oxidation by the Tet family of enzymes leads to 5-formyl-cytosine (5fC), followed by 5-carboxy-cytosine (5caC) (Fig. 1). In the second, 5hmC is deaminated by the

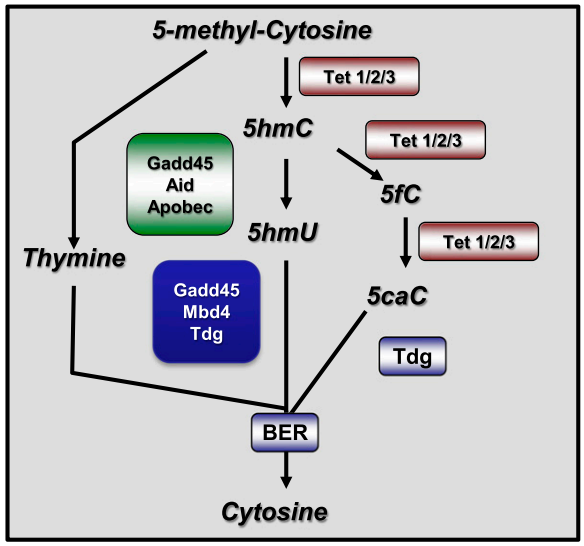

Figure 1—Illustration shows the known activated DNA demethylation pathways intermediates and their supporting enzymatic machinery. BER, base excision repair.

Gadd45/Aid/Apobec complex to form 5-hydroxymethyl-uracil (5hmU) (38). In all of these mentioned mechanisms, thymine DNA glycosylase (Tdg), a base excision repair enzyme, removes the modified base leaving an apurinic/apyrimidinic site. Concomitantly, when thymine or 5hmU are to be excised, Tdg appears to act in concert with Gadd45 and methyl CpG–binding domain protein 4 (Mbd4) (35). Lastly, the apurinic/apyrimidinic site is recognized and repaired by the base excision repair or nucleotide excision repair machinery, resulting in the replacement of an unmodified cytidine (32,34). In this report, we demonstrate that the Tet family of enzymes is activated by HG, which correlates with activated DNA demethylation. In addition, we provide evidence that the poly(ADP-ribose) polymerase (Parp) family of enzymes may initiate the demethylation cascade/s.

RESEARCH DESIGN AND METHODS

Zebrafish Husbandry, HG Induction, and Fasting Blood Glucose Determination

All procedures were performed following the guidelines described in "Principles of Laboratory Animal Care" (National Institutes of Health publication No. 85-23, revised 2011) and the approved institutional animal care and use committee animal protocol 08-19. The maintenance of zebrafish (*Danio rerio*) stocks, the induction of HG, and fasting blood glucose (FBG) determinations were performed as previously described (7,39,40).

Fish were anesthetized by placing them in 1:1000 2-phenoxyethanol for 1–2 min. For intraperitoneal injection, an insulin syringe with a 28.5-gauge needle was used to deliver 0.3% streptozotocin (S0130; Sigma-Aldrich) solution in 5 mmol/L citrate buffer (pH 5.0) to a dose of 350 mg/kg (70–150 μL, dependent on weight). Control fish were injected with a like volume of citrate buffer.

Although HG is detected within 24 h of the first injection, to induce a prolonged state of very high HG, the zebrafish require a frequent injection induction phase, followed by weekly maintenance injections as follows: week 1: three injections (day 1, 3, and 5); week 2: one injection (day 12); week 3: one injection (day 19). Blood glucose levels were determined by fasting a subset of each group for 24 h before blood collection. At this point, the fish were killed, and blood was collected after excision of the zebrafish head at the level of the anterior heart. Blood (1–2 μL) was collected from each fish, and glucose levels were determined via the QuantiChrom Glucose Assay (DIGL-200, BioAssay Systems) (40).

Parp Inhibition Protocol and Fin Regeneration Experiments

Parp activity was inhibited by an intraperitoneal injection of 1,5-isoquinolinediol (I138, Sigma-Aldrich), which has been previously used in DM rat studies (3 mg/kg) (41). Several different injection regimens were used (data not shown), and we determined for the studies presented here that the best course was to administer the inhibitor (6 mg/kg) 24 h after the streptozocin (STZ) injection during the induction phase. As such, inhibitor injections were performed at days 2, 4, and 6 relative to the beginning STZ injection as day 1. During the maintenance phase of DM, two injections per week were given at days 10, 13, 17, and 20. The tissue regeneration capacity was determined at day 22 by the procedures that we have previously published (40).

DNA, RNA, and Protein Extractions

In this study, samples were generated from 20 pooled fins, and at least three independent samples were prepared for each condition. The DNA and RNA samples were generated as we have previously described (7). Nuclear extracts of proteins were prepared via the EpiQuik Nuclear Extraction Kit (Epigentek, Farmingdale, NY) following the manufacturer's protocol without exception. For the initial homogenization step, the samples were placed in a 2-mL Dounce homogenizer, where 20 strokes with the A pestle was followed by 20 strokes with the B pestle before the remainder of the procedure was performed.

DNA, RNA, and Protein Assays

We have previously described the techniques used for quantitative (q)-RT-PCR and genome-wide DNA methylation analysis (7). As in our previous report, the DNA methylation sequencing procedure was performed by Arraystar (Rockville, MD). During preliminary foundation experiments, suitable reference genes (Supplementary Table 1) were identified, and each oligomer pair was tested to ensure that the amplification efficiency was ~100% (data not shown). In all cases, the three stable reference genes listed were used for normalization in each experiment. The ΔΔCt method (42) was used to determine the relative expression difference in the experimental samples compared with controls (43). Each sample was assayed in triplicate (technical replicates), and an average was generated. These values from three samples were used to generate the mean for each gene at each time point, and comparison with control samples yielded the fold-change reported. The sequence of the primers used for the RT-PCR studies is listed in Supplementary Table 1. The MethylFlash Hydroxymethylated DNA Quantification Kit (Colorimetric) and MethylFlash 5-Formylcytosine (5-fC) DNA Quantification Kit (Colorimetric; Epigentek) were used for the quantitation of 5hmC and 5fC, respectively. A total of 200 ng input DNA was used for the detection of 5hmC, and 500 ng input DNA was used for the detection of 5fC. As above, each sample was assayed in triplicate (at a minimum), and the 5mC derivative content reported is the average for at least three samples.

The effect of 1,5-isoquinolinediol on the methylation status of several loci we have previously reported (7) was examined via a methylated DNA immunoprecipitation, followed by q-PCR (Me-Dip-qPCR). Briefly, triplicate genomic DNA samples of control, DM, and DM and 1,5-isoquinolinediol were sonicated with a Branson Sonifier (Fisher Scientific, Pittsburgh, PA), such that >90% of the fragments were <500 bp. The samples were normalized by performing q-PCR (SYBER Green, Life Technologies Corporation, Carlsbad, CA) with primer pairs to three different genes (abhd12, uba2, and uhfr1). The samples were considered normalized once Ct values were within experimental error for each of the primer sets. Methylated DNA was then isolated from each normalized sample via immunoprecipitation using the MethylMiner kit (Life Technologies Corporation). The capture reaction protocol for 1 μg was followed without exception, and the methylated DNA was eluted via the single-fraction elution procedure.

The resultant DNA was precipitated overnight at −80°C and resuspended in 60 μL water. Two microliters were used as the template in triplicate q-PCR reactions. The primers used are listed in Supplementary Table 2 and were generated from the Zv8 genome build. The reactions were normalized to an 18S reference sequence, the values obtained from triplicate samples were averaged, and the SE was determined. Examination of Tet enzyme activity was performed by using the Epigenase 5mC-Hydroxylase TET Activity/Inhibition Assay Kit (Colorimetric; Epigentek) with the nuclear extracts generated above. Again, each sample was assayed in triplicate at a minimum.

Statistical Analysis

Student *t* test and ANOVA analysis were used where appropriate and are indicated in the figure legends.

RESULTS

HG Induces the Expression of Enzymes in the DNA Demethylation Pathways

This study was initiated by examining the HG effects on expression levels of several enzymes reported to play a role in DNA demethylation. Here, HG was induced in a group of fish, and within 24 h FBG levels increased from ~60 mg/dL

to 120 mg/dL, and by 1 week these levels increased to ~315 mg/dL, which was maintained throughout the duration of the study. At 24 h, 1, 2, and 3 weeks after induction, triplicate samples were used for RNA isolation and gene expression analysis. In all cases where statistical changes existed between control and experiment groups, the values for P were <0.001. At 24 h after induction, there were no statistically significant changes in the expression of any of the genes assayed. In contrast, the data indicate that HG induces the expression of the *tet* family and, *gadd45* members by 1 week and that these levels remain elevated throughout the experimental time course (Fig. 2). The expression of *tdg* is similar for weeks 2 and 3, but no increase was observed after week 1. In contrast, we could not detect transcriptional increases for the *abopec* family members or the T-to-G–specific binding protein *mbd4*. To firmly establish a link between HG and *tet* expression, Tet enzyme activity was determined in protein extracts from control and week 2 DM fish. In control fish samples, Tet activity was virtually undetectable (0.0023 ± 0.0012 ng/min/mg), but this increased dramatically to 1.42 ± 0.113 ng/min/mg in samples from week 2 DM fish ($n = 8$, $P < 1E\text{-}8$). As a result of these data, we examined the contribution that the *tet* family of enzymes may play in HG-induced demethylation.

HG Induces 5mC Demethylation Intermediates Consistent With Tet Enzyme Activity

As seen in Fig. 1, the initial steps of demethylation produce 5hmC if the pathway proceeds via the Tet family of enzymes. Triplicate groups of control or DM fish were generated, and genomic DNA was isolated from pooled fins at 24 h, 1 week, 2 weeks, or 3 weeks after induction (Fig. 3*A*). These samples were then examined for the presence of 5hmC; at all time points, control fish had low but detectable levels of 5hmC (0.106 ± 0.023 ng/0.2 mg), and no significant differences were observed in DM fish after 24 h (data not shown). However by 1 week, DNA exhibited significant ($P < 0.0001$) increases in the 5hmC content (1.13 ± 0.19 ng/0.2 mg). These levels continued to increase until 2 weeks (3.58 ± 0.19 ng/0.2 mg), at which time the levels were maintained, but no further increase was observed at 3 weeks (3.64 ± 0.26 ng/0.2 mg). In all cases, the FBG levels were determined for these fish, and as we previously reported, HG was induced within the first 24 h and then maintained throughout the duration of the experiment (40).

Next, studies were performed to determine if *1*) iterative oxidation, *2*) deamination first, or *3*) both pathways (Fig. 1) were subsequently used for demethylation. 5hmC is converted into 5fC in the next step of the iterative oxidation pathway, and as such, the above samples were examined for the presence of 5fC. In parallel with the 5hmC data, there was no statistical difference in the 5fC content at any time point for control fish or for fish 24 h after induction (data not shown). However, at the later time points, increases in 5fC content were observed within 1 week of HG (compare control, 0.26 ± 0.13 ng/0.5 mg vs. 1 week, 1.25 ± 0.23 ng/0.5 mg) were further increased at 2 weeks (3.1 ± 0.45 ng/0.5 mg), and maintained at 3 weeks (3.45 ± 0.22 ng/0.5 mg; Fig. 3*B*).

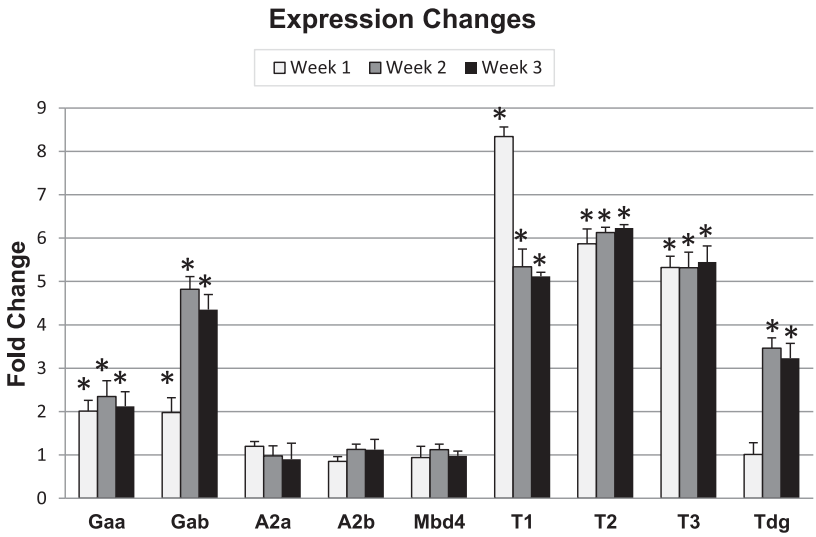

Figure 2—HG induces gene expression changes in DNA demethylation machinery enzymes. Quantitative reverse transcriptase results (with SE) are presented graphically as the fold increase when compared with controls for weeks 1–3, respectively: Gaa (*gadd45* αα): 2.01 ± 0.25, 2.35 ± 0.36, and 2.12 ± 0.34; Gab (*gadd45* αβ): 1.98 ± 0.34, 4.82 ± 0.29, and 4.35 ± 0.35; A2a (*apobec2a*): 1.20 ± 0.11, 0.98 ± 0.23, and 0.90 ± 0.37; A2b (*apobec2b*): 0.85 ± 0.11, 1.13 ± 0.12, and 1.12 ± 0.24; Mbd4 (*mbd4*): 0.94 ± 0.26, 1.12 ± 0.13, and 0.98 ± 0.11; T1 (*tet 1*): 8.34 ± 0.22, 5.34 ± 0.41, and 5.12 ± 0.09; T2 (*tet 2*): 5.87 ± 0.34, 6.13 ± 0.12, and 6.23 ± 0.08; T3 (*tet 3*): 5.32 ± 0.26, 5.32 ± 0.36, and 5.45 ± 0.37; and Tdg (*tdg*): 1.01 ± 0.27, 3.46 ± 0.24, and 3.23 ± 0.34. Each gene at each time point was compared with the appropriate control, and a Student *t* test was performed to determine statistical significance. *$P < 0.001$ (indicating statistically significant changes existed).

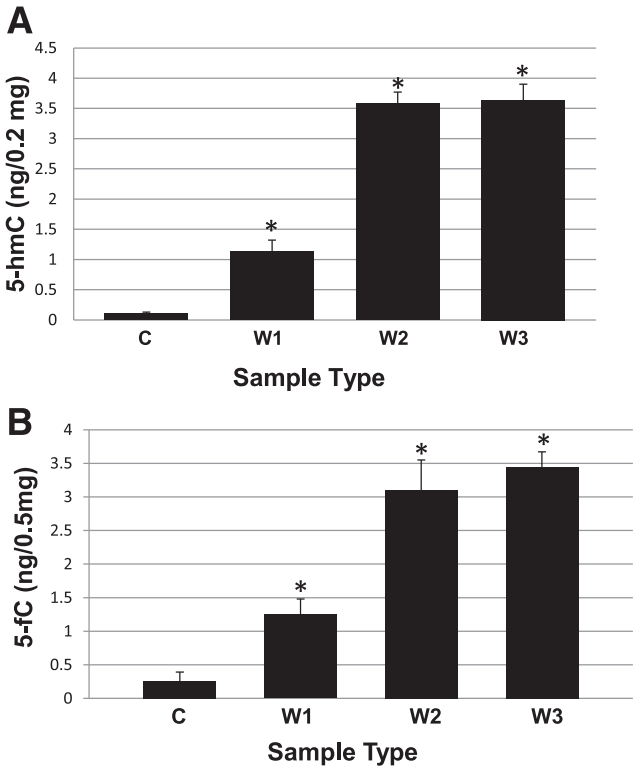

Figure 3—HG induces the formation of Tet enzyme activity intermediates. *A*: Graphic representation of the 5hmC genomic content (ng/0.2 mg); control (C): 0.106 ± 0.023, W1 (week 1): 1.13 ± 0.19, W2 (week 2): 3.58 ± 0.19, W3 (W3): 3.64 ± 0.26 (n = 18 for C, W1, and W2; n = 16 for W3). *B*: Graphic representation showing the time course of 5fC formation (ng/0.5 mg) induced in fin tissue DNA. Control (C): 0.26 ± 0.13, W1: 1.25 ± 0.23, W2: 3.1 ± 0.45, and W3: 3.45 ± 0.22 (n = 18 for C, W1 and W2; n = 16 for W3). $P <$ 0.0001. In both studies, a Student t test was performed to determine statistical significance. *$P <$ 0.0001 (indicating statistically significant changes existed). In addition, a one-way ANOVA analysis revealed that week 1 was statistically different than weeks 2 and 3 ($P <$ 1.0 E-5 for both assays).

The other pathway that 5hmC may follow is deamination by the Aid/Apobec enzymes, yielding as an initial step 5-hydroxymethyl-uracil (5hmU; Fig. 1). Despite repeated attempts to detect 5hmU with antibodies from a variety of vendors that could detect commercially purchased 5hmU, we were not able to detect this derivative in control or DM samples (data not shown).

Parp1 Inhibition Prevents DNA Demethylation

A recent study reported that Parp1 activity is necessary for the upregulation of Tet1 expression, which in turn, is responsible for the initiation of active demethylation in mouse primordial germ cell DNA during development (44). We therefore determined the role that Parp plays in the HG-induction of DNA demethylation. We took advantage of the temporal window observed between HG induction and the induction of DNA demethylation by injecting control and DM fish with an inhibitor of the Parp enzymes. Subsequent to this, DNA was extracted and examined for its 5hmC content. As can be seen in Fig. 4*A*, DM induced the conversion of 5mC into 5hmC (compare control: 0.099 ± 0.033 ng/0.2 mg vs. DM: 3.51 ± 0.32 ng/0.2 mg), which was completely prevented by the inclusion of the Parp inhibitor 1,5 isoquinolinediol (DM and Parp inhibitor: 0.073 ± 0.039 ng/0.2 mg). In addition, the 1,5 isoquinolinediol treatment had no effects on HG because the doubly treated group had similar FBG levels as DM fish (~315 mg/dL for both groups; data not shown).

To further support these data, we examined the effect that Parp inhibition had on loci that we used in our previous study (7) via a MeDip-qPCR approach. These included loci that are unaffected by HG, remaining fully methylated (abhd12, map1b) or fully unmethylated (uba2, rac3a), and more importantly, loci that are demethylated in response to HG (uhrf1, grtp1a, gcat, hnrnpa0). As expected, the loci that are not affected by HG exhibit equal amounts of methylation, as indicated by equal

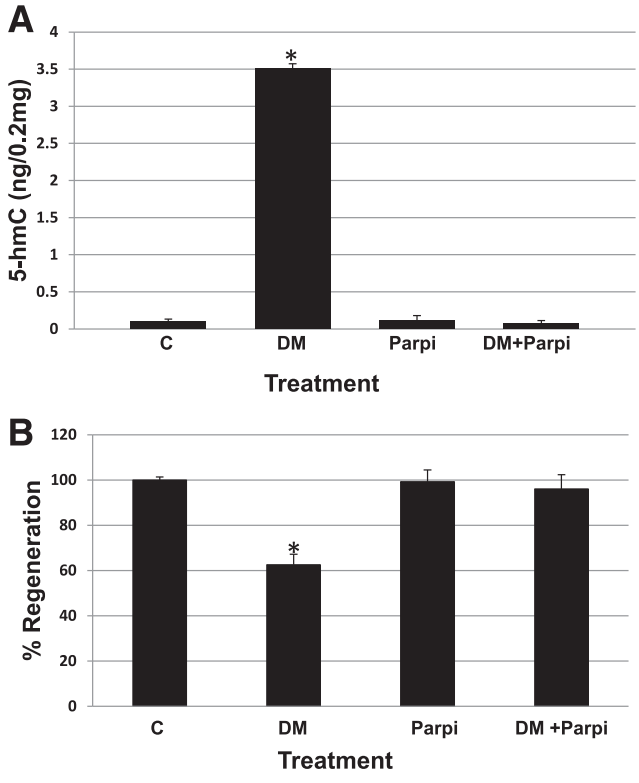

Figure 4—Parp inhibition prevents both the accumulation of 5hmC and the HG-induced fin regeneration deficit. *A*: The administration of a Parp inhibitor (Parpi) prevents 5hmC formation (ng/0.2 mg). Control (C): 0.099 ± 0.033, DM: 3.51 ± 0.32, Parpi: 0.007 ± 0.003, and DM+Parpi: 00.073 ± 0.039 (n = 8). *$P <$ 1.0 E-6 (indicating that only DM samples were statistically different from the other samples by one-way ANOVA analysis). *B*: Parp inhibition prevents the HG-induced impairment in fin regeneration. Control (C): 100 ± 1.3%, DM: 62.5 ± 4.7%, Parpi: 99.3 ± 5.2%, and DM+Parpi: 96.3 ± 6.3% (n = 18 for all groups). *$P <$ 5.0 E-5 (indicating that the regeneration of only DM fish were statistically different from the other samples by a one-way ANOVA analysis).

q-PCR Ct values irrespective of the sample origin (Table 1). In contrast, the Ct values for HG-affected loci are significantly lower in the DM samples than in all others, thus indicating that the inclusion of Parp inhibitor prevented DNA demethylation.

In our previous work, we documented that HG causes an impairment of tissue regeneration and that impairment correlated with the induction of DNA demethylation (7). After observing that Parp inhibition appears to prevent the *tet*-dependent pathway(s) of demethylation, we examined if this inhibition also restored regenerative capacity of the fin. As such, the rate of tissue regeneration was documented for the fish used in the DNA extraction experiment documented above. In these experiments, the regeneration of control fish and fish injected with Parp inhibitor and DM plus Parp inhibitor all exhibited normal levels of regeneration (control: 100%, Parp: 99.25%, DM plus Parp inhibitor, 96.29%; Fig. 4*B* and Supplementary Fig. 1). This is in contrast with DM fish, which exhibited a reduced fin regeneration rate (62.5%) similar to our previous reports (40).

DISCUSSION

Epigenetic mechanisms are hypothesized to play a role in the MM phenomena because they provide a mechanism for continued altered gene expression without the presence of the initiating HG stimulus (45). We and others have reported that HG can induce site-specific DNA methylation, and we have also reported that these changes persist even after euglycemia is restored in a zebrafish model of type 1 DM (7). In this report we have revealed a role for the Tet family of enzymes in HG-induced DNA demethylation. More specifically, we provide evidence that HG induces the expression and activity of the Tet enzymes, yielding known intermediates of the iterative oxidation pathway leading to the demethylation of 5mC. In addition, these studies have revealed that demethylation via this pathway can be prevented through inhibiting the Parps.

We initiated this study by examining the HG effects on expression of enzymes known to play key roles in each of the DNA demethylation pathways. In regard to the deamination first pathway, where 5mC is converted to thymine, we observed increased expression for the adaptor Gadd45 protein but no increase in the Aid/Apobec complex or the Mbd4 protein. Mbd4 appears to be critical for this pathway because it has been shown that Mbd4 recognizes and excises mismatched bases paired with guanine (G:X), where X is uracil, thymine, or 5hmU (46). On the surface, these data might suggest that HG may not induce this pathway; however, we cannot make this conclusion without additional data regarding the presence of T:G mismatches. Unfortunately, we were unable to pursue this pathway further because no efficient means are available for examination of these processes or the ability to examine Mbd4 activity specifically. The other two pathways are both initiated by the Tet family of enzymes, and our data clearly revealed an increase in the expression of these enzymes within 2 weeks of hyperglycemic onset. This expression increase was supported by the correlated increase in Tet enzymatic activity. In addition, the expression of the Tdg enzyme (a base excision repair enzyme), which is responsible for removal of the modified base in these pathways, is also increased.

We next examined DNA from the control and DM groups for known intermediates of the demethylation pathways. The common intermediate for the Tet-specific demethylation pathway(s) is 5hmC, and the data presented here reveal that by 2 weeks of HG, 5hmC levels are maximized and maintained at ~30-fold higher levels than in control fish. These data correspond perfectly with the caudal fin regeneration deficit we have previously reported, in that at 2 weeks, the HG-induced deficit reaches its maximum and is maintained in subsequent weeks (40). After 5hmC formation, cytosine demethylation can proceed via two routes, either through deamination or iterative oxidation, and each of these pathways produces different intermediates. The next step in the iterative oxidation pathway is the production of 5fC. We were able to detect significant increases in this intermediate, as expected, due to the increase in Tet enzyme activity,

Table 1—Parp inhibition prevents DNA demethylation as determined by q-PCR results

Locus	Control	DM	DM+I	I
abhd12	21.0 ± 0.21	20.8 ± 0.34	21.6 ± 0.56	20.7 ± 0.76
map1b	20.4 ± 0.44	20.1 ± 0.36	19.7 ± 0.66	20.4 ± 0.66
uba2	36.8 ± 2.69	37.9 ± 3.75	36.3 ± 2.66	39.4 ± 4.78
rac3af	38.9 ± 4.20	40.9 ± 2.33	40.3 ± 3.56	40.6 ± 4.14
uhrf1	21.0 ± 0.41	36.3 ± 2.45*	22.7 ± 1.98	20.9 ± 1.65
grtp1a	25.6 ± 0.18	30.1 ± 0.20*	24.9 ± 0.38	25.2 ± 0.65
gcat	24.8 ± 0.21	29.0 ± 0.17*	24.4 ± 0.21	23.9 ± 0.41
hnrnpa0	26.4 ± 0.67	36.0 ± 0.89*	27.4 ± 0.67	27.6 ± 0.97

The gene loci are indicated, and the average Ct values and their associated SE are reported for control, DM, DM plus Parp inhibitor (DM+I), and Parp inhibitor (I) injected fish. Statistical significance was determined by a one-way ANOVA analysis. *$P < 0.01$ (indicating statistically significant differences).

and as such, our data are consistent with HG-induced DNA demethylation proceeding, at least in part, via the *tet*-dependent iterative oxidation pathway. Unfortunately, we were unable to detect 5hmU in any of our samples and cannot rule in/out the use of this pathway.

In the context of DM, Parp1 senses HG-induced DNA damage and plays a pivotal role in stimulating the molecular pathways that underlie all diabetes complications (20). This fact, coupled with the report linking Parp1 activity and upregulation of Tet1 expression, led us to hypothesize that inhibition of the Parp enzymes may prevent Tet activity. When a known Parp enzyme inhibitor was included in our experiments, the levels of 5hmC returned to normal. In addition, enzyme inhibition also prevented the demethylation of several specific loci examined. Several recent reports have documented that Parp inhibition can ameliorate renal hypertrophy, podocyte apoptosis, and peripheral neuropathy in animal models of DM (47–49). When we examined the effect Parp inhibition had on tissue regeneration, we observed a complete restoration of the regenerative capacity in DM fish that were also treated with the Parp inhibitor. These data provide further evidence that Parp inhibition may provide a therapeutic avenue for the prevention or reversal of diabetes complications and also illustrates the usefulness of the zebrafish model for small-molecule drug discovery pertaining to DM.

From a mechanistic perspective, our data are consistent with the HG induction of the Parp family of enzymes, which in turn stimulates the Tet enzymes leading to DNA demethylation and ultimately persistent diabetes complications.

Funding. This work was supported by a research grant from The Iacocca Family Foundation, Rosalind Franklin University start-up funds, and National Institutes of Health grant DK-092721 awarded to R.V.I.

Duality of Interest. No potential conflicts of interest relevant to this article were reported.

Author Contributions. N.D. researched the data and discussed the data. M.P.S. contributed to discussion of the data and writing the manuscript. E.L. and S.M.M. provided technical support. R.V.I. researched and discussed the data and contributed to writing and editing the manuscript. R.V.I. is the guarantor of this work and, as such, had full access to all the data in the study and takes responsibility for the integrity of the data and the accuracy of the data analysis.

References

1. Shaw JE, Sicree RA, Zimmet PZ. Global estimates of the prevalence of diabetes for 2010 and 2030. Diabetes Res Clin Pract 2010;87:4–14

2. Engerman RL, Kern TS. Progression of incipient diabetic retinopathy during good glycemic control. Diabetes 1987;36:808–812

3. Hammes HP, Klinzing I, Wiegand S, Bretzel RG, Cohen AM, Federlin K. Islet transplantation inhibits diabetic retinopathy in the sucrose-fed diabetic Cohen rat. Invest Ophthalmol Vis Sci 1993;34:2092–2096

4. Kowluru RA. Effect of reinstitution of good glycemic control on retinal oxidative stress and nitrative stress in diabetic rats. Diabetes 2003;52:818–823

5. Kowluru RA, Chakrabarti S, Chen S. Re-institution of good metabolic control in diabetic rats and activation of caspase-3 and nuclear transcriptional factor (NF-kappaB) in the retina. Acta Diabetol 2004;41:194–199

6. Li SL, Reddy MA, Cai Q, et al. Enhanced proatherogenic responses in macrophages and vascular smooth muscle cells derived from diabetic db/db mice. Diabetes 2006;55:2611–2619

7. Olsen AS, Sarras MP Jr, Leontovich A, Intine RV. Heritable transmission of diabetic metabolic memory in zebrafish correlates with DNA hypomethylation and aberrant gene expression. Diabetes 2012;61:485–491

8. Nathan DM, McGee P, Steffes MW, Lachin JM; DCCT/EDIC Research Group. Relationship of glycated albumin to blood glucose and HbA1c values and to retinopathy, nephropathy, and cardiovascular outcomes in the DCCT/EDIC study. Diabetes 2014;63:282–290

9. The Diabetes Control and Complications Trial/Epidemiology of Diabetes Interventions and Complications Research Group. Retinopathy and nephropathy in patients with type 1 diabetes four years after a trial of intensive therapy. Am J Ophthalmol 2000;129:704–705

10. UK Prospective Diabetes Study (UKPDS) Group. Intensive blood-glucose control with sulphonylureas or insulin compared with conventional treatment and risk of complications in patients with type 2 diabetes (UKPDS 33). Lancet 1998; 352:837–853

11. Turner RC, Cull CA, Frighi V, Holman RR; UK Prospective Diabetes Study (UKPDS) Group. Glycemic control with diet, sulfonylurea, metformin, or insulin in patients with type 2 diabetes mellitus: progressive requirement for multiple therapies (UKPDS 49). JAMA 1999;281:2005–2012

12. Gaede PH, Jepsen PV, Larsen JN, Jensen GV, Parving HH, Pedersen OB. The Steno-2 study. Intensive multifactorial intervention reduces the occurrence of cardiovascular disease in patients with type 2 diabetes. Ugeskr Laeger 2003;165: 2658–2661 [in Danish]

13. Holman RR, Paul SK, Bethel MA, Matthews DR, Neil HA. 10-year follow-up of intensive glucose control in type 2 diabetes. N Engl J Med 2008;359:1577–1589

14. Ismail-Beigi F, Craven T, Banerji MA, et al.; ACCORD trial group. Effect of intensive treatment of hyperglycaemia on microvascular outcomes in type 2 diabetes: an analysis of the ACCORD randomised trial. Lancet 2010;376:419–430

15. Duckworth WC, McCarren M, Abraira C; VA Diabetes Trial. Glucose control and cardiovascular complications: the VA Diabetes Trial. Diabetes Care 2001;24: 942–945

16. Skyler JS, Bergenstal R, Bonow RO, et al.; American Diabetes Association; American College of Cardiology Foundation; American Heart Association. Intensive glycemic control and the prevention of cardiovascular events: implications of the ACCORD, ADVANCE, and VA diabetes trials: a position statement of the American Diabetes Association and a scientific statement of the American College of Cardiology Foundation and the American Heart Association. Diabetes Care 2009;32:187–192

17. Riddle MC. Effects of intensive glucose lowering in the management of patients with type 2 diabetes mellitus in the Action to Control Cardiovascular Risk in Diabetes (ACCORD) trial. Circulation 2010;122:844–846

18. The Diabetes Control and Complications Trial Research Group. The effect of intensive treatment of diabetes on the development and progression of long-term complications in insulin-dependent diabetes mellitus. N Engl J Med 1993;329: 977–986

19. Ihnat MA, Thorpe JE, Kamat CD, et al. Reactive oxygen species mediate a cellular 'memory' of high glucose stress signalling. Diabetologia 2007;50: 1523–1531

20. Ceriello A, Ihnat MA, Thorpe JE. Clinical review 2: The "metabolic memory": is more than just tight glucose control necessary to prevent diabetic complications? J Clin Endocrinol Metab 2009;94:410–415

21. Morgan HD, Sutherland HG, Martin DI, Whitelaw E. Epigenetic inheritance at the agouti locus in the mouse. Nat Genet 1999;23:314–318

22. Ling C, Del Guerra S, Lupi R, et al. Epigenetic regulation of PPARGC1A in human type 2 diabetic islets and effect on insulin secretion. Diabetologia 2008; 51:615–622

23. Caramori ML, Kim Y, Moore JH, et al. Gene expression differences in skin fibroblasts in identical twins discordant for type 1 diabetes. Diabetes 2012;61: 739–744
24. Zhao J, Goldberg J, Bremner JD, Vaccarino V. Global DNA methylation is associated with insulin resistance: a monozygotic twin study. Diabetes 2012;61: 542–546
25. Sapienza C, Lee J, Powell J, et al. DNA methylation profiling identifies epigenetic differences between diabetes patients with ESRD and diabetes patients without nephropathy. Epigenetics 2011;6:20–28
26. Akirav EM, Lebastchi J, Galvan EM, et al. Detection of β cell death in diabetes using differentially methylated circulating DNA. Proc Natl Acad Sci U S A 2011;108:19018–19023
27. Toperoff G, Aran D, Kark JD, et al. Genome-wide survey reveals predisposing diabetes type 2-related DNA methylation variations in human peripheral blood. Hum Mol Genet 2012;21:371–383
28. Rakyan VK, Beyan H, Down TA, et al. Identification of type 1 diabetes-associated DNA methylation variable positions that precede disease diagnosis. PLoS Genet 2011;7:e1002300
29. Volkmar M, Dedeurwaerder S, Cunha DA, et al. DNA methylation profiling identifies epigenetic dysregulation in pancreatic islets from type 2 diabetic patients. EMBO J 2012;31:1405–1426
30. Williams KT, Garrow TA, Schalinske KL. Type I diabetes leads to tissue-specific DNA hypomethylation in male rats. J Nutr 2008;138:2064–2069
31. Pirola L, Balcerczyk A, Tothill RW, et al. Genome-wide analysis distinguishes hyperglycemia regulated epigenetic signatures of primary vascular cells. Genome Res 2011;21:1601–1615
32. Wu SC, Zhang Y. Active DNA demethylation: many roads lead to Rome. Nat Rev Mol Cell Biol 2010;11:607–620
33. Williams KT, Schalinske KL. Tissue-specific alterations of methyl group metabolism with DNA hypermethylation in the Zucker (type 2) diabetic fatty rat. Diabetes Metab Res Rev 2012;28:123–131
34. Moore LD, Le T, Fan G. DNA methylation and its basic function. Neuropsychopharmacology 2013;38:23–38
35. Niehrs C, Schäfer A. Active DNA demethylation by Gadd45 and DNA repair. Trends Cell Biol 2012;22:220–227
36. Ito S, D'Alessio AC, Taranova OV, Hong K, Sowers LC, Zhang Y. Role of Tet proteins in 5mC to 5hmC conversion, ES-cell self-renewal and inner cell mass specification. Nature 2010;466:1129–1133
37. Tahiliani M, Koh KP, Shen Y, et al. Conversion of 5-methylcytosine to 5-hydroxymethylcytosine in mammalian DNA by MLL partner TET1. Science 2009;324:930–935
38. Guo JU, Su Y, Zhong C, Ming GL, Song H. Emerging roles of TET proteins and 5-hydroxymethylcytosines in active DNA demethylation and beyond. Cell Cycle 2011;10:2662–2668
39. Intine RV, Olsen AS, Sarras MP Jr. A zebrafish model of diabetes mellitus and metabolic memory. J Vis Exp 2013;Feb 28:e50232
40. Olsen AS, Sarras MP Jr, Intine RV. Limb regeneration is impaired in an adult zebrafish model of diabetes mellitus. Wound Repair Regen 2010;18:532–542
41. Lupachyk S, Shevalye H, Maksimchyk Y, Drel VR, Obrosova IG. PARP inhibition alleviates diabetes-induced systemic oxidative stress and neural tissue 4-hydroxynonenal adduct accumulation: correlation with peripheral nerve function. Free Radic Biol Med 2011;50:1400–1409
42. Lan CC, Tang R, Un San Leong I, Love DR. Quantitative real-time RT-PCR (qRT-PCR) of zebrafish transcripts: optimization of RNA extraction, quality control considerations, and data analysis. Cold Spring Harb Protoc 2009;2009:pdb. prot5314
43. Sarras MP Jr, Leontovich AA, Olsen AS, Intine RV. Impaired tissue regeneration corresponds with altered expression of developmental genes that persists in the metabolic memory state of diabetic zebrafish. Wound Repair Regen 2013;21:320–328
44. Ciccarone F, Klinger FG, Catizone A, et al. Poly(ADP-ribosyl)ation acts in the DNA demethylation of mouse primordial germ cells also with DNA damage-independent roles. PLoS ONE 2012;7:e46927
45. Intine RV, Sarras MP Jr. Metabolic memory and chronic diabetes complications: potential role for epigenetic mechanisms. Curr Diab Rep 2012;12:551–559
46. Hashimoto H, Zhang X, Cheng X. Excision of thymine and 5-hydroxymethyluracil by the MBD4 DNA glycosylase domain: structural basis and implications for active DNA demethylation. Nucleic Acids Res 2012;40:8276–8284
47. Drel VR, Pacher P, Stavniichuk R, et al. Poly(ADP-ribose)polymerase inhibition counteracts renal hypertrophy and multiple manifestations of peripheral neuropathy in diabetic Akita mice. Int J Mol Med 2011;28:629–635
48. Jangra A, Datusalia AK, Khandwe S, Sharma SS. Amelioration of diabetes-induced neurobehavioral and neurochemical changes by melatonin and nicotinamide: implication of oxidative stress-PARP pathway. Pharmacol Biochem Behav 2013;114–115:43-51
49. Peixoto EB, Papadimitriou A, Lopes de Faria JM, Lopes de Faria JB. Tempol reduces podocyte apoptosis via PARP signaling pathway in experimental diabetes mellitus. Nephron, Exp Nephrol 2012;120:e81–e90